IEEE Access
Multidisciplinary ⋮ Rapid Review ⋮ Open Access Journal

Received 4 March 2025, accepted 24 March 2025, date of publication 9 April 2025, date of current version 8 May 2025.

Digital Object Identifier 10.1109/ACCESS.2025.3558750

RESEARCH ARTICLE

Performance and Cost of Dynamic Reliability: A 6G Industrial Environment Perspective

GIANLUCA DAVOLI [1,2], (Member, IEEE), FEDERICO TONINI [1], (Member, IEEE), DAVIDE BORSATTI [1,2], (Member, IEEE), WINT YI POE [3], RICCARDO TRIVISONNO [3], (Senior Member, IEEE), AND WALTER CERRONI [1,2], (Senior Member, IEEE)

[1]CNIT WiLab, 40133 Bologna, Italy
[2]DEI, University of Bologna, 40136 Bologna, Italy
[3]Huawei Technologies, 80992 Munich, Germany

Corresponding author: Walter Cerroni (walter.cerroni@unibo.it)

This work was supported by the Huawei - National Inter-university Consortium for Telecommunications (Huawei-CNIT) Joint Innovation Center (JIC).

ABSTRACT The use of robots in modern manufacturing facilities, where also human workers operate, offers substantial advantages, but also introduces safety hazards that need to be mitigated with all possible means. Ultra-reliable communication services offered by 5G mobile networks allow for automated remote control of the machines, thus enabling a new generation of network applications that can enforce safety procedures in a hyper-connected industrial environment. However, in the context of Human-Robot Collaboration scenarios very strict safety requirements must be satisfied, determining communication reliability levels to be guaranteed that go beyond the up to 10^{-5} capabilities of 5G ultra-reliable deployments. Moreover, in 5G the reliability is imposed as fixed requirement to be achieved at all times, which may lead to resource overprovisioning. Resource efficiency can be improved by dynamically adapting the target network reliability level based on the actual needs of the connected devices, still guaranteeing safe human-robot interactions. The idea of dynamic reliability applied to 6G industrial environments, introduced in our previous work, is further investigated in this paper by evaluating performance and costs of the approach, and by exploring how to leverage the knowledge of the specific nature of the task performed by robots cooperating with humans. The results of our study allow to quantify the resource gain that can be achieved with dynamic reliability compared to the solution currently offered by 5G systems, as well as the cost that must be factored in in terms of network signalling overhead.

INDEX TERMS 6G, dynamic reliability, human–robot collaboration, industrial networks, task awareness in automated manufacturing.

I. INTRODUCTION

The integration of robots into industrial workflows has dramatically transformed manufacturing and logistics processes, bringing about significant improvements in productivity, precision, and efficiency. On the other hand, this has also introduced specific safety challenges that must be addressed to protect the well-being of human workers operating in the same space as robots. Communication and networking technologies can significantly help addressing those challenges, enabling accurate and real-time monitoring and control features in the workplace [1]. As industries continue to embrace automation and robotics to support progressively more demanding use-cases, the necessity for advanced and highly reliable communication systems becomes increasingly evident. The advent of 5G networks began to meet this need by providing support to Ultra-Reliable Low-Latency Communications (URLLC) services. Nonetheless, the evolving industrial environments introduce new challenging operational modes, such as Human-Robot Collaboration (HRC), where human workers share the workspace with robots while performing some specific tasks

The associate editor coordinating the review of this manuscript and approving it for publication was Tarcisio Ferreira Maciel.

collaboratively. This can lead to monitoring and control scenarios with stricter requirements in terms of reliable communications that go beyond what is currently offered by 5G deployments [2], such as those identified in the Hyper Reliable and Low-Latency Communications (HRLLC) by ITU-R for the IMT-2030 (6G) use case [3].

Among other target key performance indicators, 6G networks are expected to achieve at least a "two-nine" increase (up to $1 \cdot 10^{-7}$) in supported communication reliability with reference to that offered by 5G systems, with the same number of users and access points for unit area [3] [4]. A way to reach that target would consist in taking advantage of increased communication resource redundancy, for instance by further increasing the number of supported replicated parallel data streams between the User Equipment (UE) and the data network, which is currently limited to two in the 5G redundant transmission approach leveraging dual connectivity [5], [6].

Meeting hyper-reliability requirements is not the only challenge for 5G. In fact, in 5G URLLC the reliability is considered a "static" attribute to be always provided. However, the constant use of multiple and always active redundant communication channels can become very demanding, not only in terms of resource usage but also in terms of energy consumption, considering as well that such parallel data streams may not be strictly necessary all the time. Sustainability, achieved by minimizing energy consumption and the use of resources, is a key capability expected in 6G [3]. Based on this observation, the concept of provisioning communication services with *dynamic reliability* for HRC scenarios was recently introduced: depending on the mutual distance between a human and a robot, or between two robots, the target reliability level of their data connections can be dynamically set to either a high or a low value, adapting the resource redundancy enforcement to the possible detection of critical safety conditions that require highly reliable monitoring and control of the robot movements [7], [8]. This approach has been proven to be beneficial in environments where humans and robots move around and hazardous conditions may arise, as it allows to save resources and, consequently, reduce energy consumption while achieving reliability levels not supported by current 5G networks [9]. However, a thorough performance analysis and evaluation of the resource gain that can be achieved with dynamic reliability is still needed, as well as an assessment of the cost introduced by the approach in terms of network signaling overhead.

Relying only on the distance between UEs to identify critical safety situations in an HRC scenario can be inefficient. In industrial settings, robots might work in fixed locations, and human workers are not necessarily at risk just because they are nearby. For instance, if a robotic arm is enclosed in protective glass and performing autonomous tasks, there is no need to allocate high-reliability communication to nearby workers. A more effective approach is to consider what tasks humans and robots are actually performing and provide redundant communication resources only when necessary. This allows to achieve *task-aware dynamic reliability*, showing how it is possible to add a new dimension to the efficient deployment of URLLC-like services in future 6G networks by taking advantage of some of the peculiarities of a given vertical application. The final objective is to have the network assist the operations within industrial environments and make the workplace safer while also efficiently using communications resources and improving the cost.

In this paper, we significantly extend our previous work on dynamic reliability [7], [8], [9], [10] by evaluating performance and costs of the approach and by exploring how to leverage the knowledge of the specific nature of the HRC tasks. In particular, the main contributions of this paper include:

- a detailed evaluation through simulation of the performance of dynamic reliability under different parameter settings, such as the number of UEs and the number of sub-areas in which the factory floor can be split to reduce the algorithm compute time;
- an evaluation of the resource gain obtained by applying dynamic reliability, i.e. the savings in terms of redundant communication channels that can be achieved by the dynamic approach with respect to the static redundant transmission mechanisms currently offered by the 5G network;
- an assessment of the additional gain that can be obtained with task-aware dynamic reliability, by factoring in the characteristics of the activities that human and robot workers are carrying out, distinguishing between *collaborative* and *autonomous* tasks;
- a simple model that allows to quantify the cost of dynamic reliability in terms of network signaling overhead, determining the minimum frequency with which the UE locations must be sampled and processed and discussing how to avoid that network reconfiguration happens too frequently.

The paper is structured as follows. Section II contextualizes the background behind this work and recalls some of the existing body of literature. Section III discusses the concept and advantages of dynamic reliability in 6G industrial environments, recalling our previous work on the subject and adding the new dimension of task awareness. Section IV includes some considerations on the feasibility of dynamic reliability in the framework of the current 5G mobile network architecture and the gaps that might be addressed in its evolution toward 6G. Sections V and VI present the results of the performance analysis and resource gain of the proposed approaches, respectively without and with task awareness. Section VII presents a simple model to quantify the network signalling overhead induced by dynamic reliability. Finally, Section VIII draws the conclusion.

II. BACKGROUND AND RELATED WORK

To motivate the need for a dynamic and task-aware approach to enforce reliable connectivity in indoor industrial access networks, we first analyze the reference HRC scenario, both in terms of entities operating in it and techniques to provide connectivity to all of them.

A. HUMAN-ROBOT COLLABORATION

The International Federation of Robotics (IFR) classifies *robot colleagues* into *industrial* and *service robots* [11]. Industrial robots handle manufacturing and material manipulation within a defined range of motion, while service robots assist with tasks like transport and cleaning, moving autonomously. The IFR also defines key human-robot collaboration types, including *Coexistence*, where they share a workspace without physical barriers but do not interact, and *Sequential collaboration*, where they take turns working in the same space.

Among the key safety risks in HRC for manufacturing goods, collision hazards and "pinch and crush" situations are amid the most prominent ones. Such hazards can lead to injuries, equipment damage, and production disruptions. For these reasons, implementing advanced sensing technologies and safety measures to detect and prevent collisions is essential.

A combination of engineering controls, administrative procedures, and personal protective measures should be implemented to mitigate these safety hazards. Safety standards and regulations, such as ISO 10218 for industrial robots and ISO/TS 15066 for collaborative robot safety, provide guidelines for designing and operating collaborative robotic systems safely. Although these guidelines still hold, in modern always-connected environments additional features can be developed and leveraged to further improve safety. For example, the low-latency and high-reliability features supported by URLLC services in mobile networks can be leveraged to collect real-time data and timely send, either reactively or proactively, "halt" signals to machines when dangerous situations are detected or predicted. This, however, requires knowing the position of both robots and humans, but also the kind of task they are performing.

In the literature, some studies describe the activities of collaborative manufacturing processes in detail, including the evolution over time of the tasks carried out by cooperating humans and robots. One such work is [12], where the authors describe the interaction of a human worker with a manufacturing robot with two arms, for the assembly of multiple printed circuit boards to be inserted into a plastic enclosure, including quality controls for the integrity of the product. They perform tasks together, sharing the same working space, with some periods of collaboration and others of autonomous work. Similarly, [13] describes collaborative tasks as tasks where there is input of material without stopping the system and interactions that can involve physical contact. In [14], the authors propose a classification for guidelines for the design of safe HRC assembly environments, validating it by means of a laboratory case study, for which a detailed description is provided, including a timeline of the interaction between workers. In this paper, we leverage the knowledge of collaborative and autonomous tasks, along with that of the position of workers, to decide on the level of reliability that the mobile network should provide, optimizing resource utilization by minimizing the amount of redundant resources to be put in place.

B. MOBILE COMMUNICATION RESOURCE ASSIGNMENT IN INDUSTRIAL SCENARIOS

Different studies provide evidence of the need for high reliability and low latency in 6G communication, especially in industrial scenarios where automated plants need real-time data transmission and operation [15]. Thanks to its support of sub-ms latency and extremely high reliability, 6G is expected to enable Industry X.0 paradigm [16], where intelligent industrial automation requires the integration of artificial intelligence algorithms for ultra-fast and reliable decision-making processes.

Industrial automation through robots requires real-time and closed-loop robot control, which can be considered part of the URLLC service class [17]. Enhanced network reliability is also crucial to provide a safe working environment for humans collaborating with robots. The paper in [18] analyzes the trade-offs between reliability and latency in industrial scenarios with strict requirements. Large data blocks with strong channel codes can be sent to ensure reliability, but this approach often results in increased transmission latency. Conversely, employing shorter block lengths can reduce latency, at the expense of degraded reliability, requiring frequent retransmissions. The paper also proposes to adopt joint optimization of data block lengths and pilot lengths to find the right trade-offs between reliability and latency. Among the large body of work on URLLC, [5] enumerates the challenges of enabling this kind of application, and proposes solutions that do not impact latency, such as multi-connectivity. In [6], the benefits of duplicating packets for URLLC applications in 5G networks are analyzed, both in terms of enhanced reliability and efficient resource usage, albeit limited to two connected paths, as per the dual connectivity feature standardized in 5G. Our recent work on multi-connectivity shows that stringent reliability requirements posed by industrial applications might require more than two parallel streams contemporarily active [7], surpassing the current 5G capabilities. Even though using multiple connections can increase communication efficacy and reliability, it has an impact on the required radio resources, especially when a static approach, i.e., a fixed number of connections over time, is used.

A way to optimize the use of network resources in industrial environments is to leverage information on robotic tasks. In [19], the authors present a joint robot path planning and radio beam scheduling to reduce interference in a mmWave industrial network, thus improving the transmission rate. In [20], the authors propose an optimization strategy that leverages the pseudo-deterministic nature of industrial robotic jobs to minimize the maximum aggregate traffic in the network. On the one hand, these works show that resource consumption can be optimized by leveraging information on robotic tasks. On the other hand, they do not consider human-robot interactions and related reliability and safety aspects.

As previously mentioned, in [7], [9] we propose using multi-connectivity to achieve target reliability levels by tuning the number of active communication channels depending on the distance between UEs, a concept referred to as dynamic reliability. We also highlight that there are situations where 5G falls short of the goal, given its limit of two connections per UE (i.e., dual connectivity). In [8], we proposed the adoption of a control entity in communication systems to support dynamic reliability for HRC. In this work, we extend our previous contributions by evaluating performance and costs of the approach, and by including information on tasks that workers are carrying out in the reliability tuning process, aiming at covering a wider set of real-world scenarios, as well as further improving resource utilization efficiency.

III. DYNAMIC RELIABILITY IN 6G INDUSTRIAL ENVIRONMENTS

A. DYNAMIC RELIABILITY BASED ON CRITICAL DISTANCE

As a relevant use case to understand the advantages offered by the concept of dynamic reliability, we consider an industrial environment where wireless connectivity services are provided by what we envision will be an indoor 6G network. A relatively large factory floor is assumed, where human workers and robots coexist and operate to manufacture goods. Each robot and each human worker carries a device (UE) connected to the network, and is free to move around the working area, which is covered by a set of Access Nodes (ANs). In the following, for the sake of brevity, we will use the term "worker" collectively for both humans and robots, when not otherwise specified. Also, we will sometimes associate the working task directly to a UE, rather than specifying "the worker that carries the UE".

When a robot gets too close to a human worker or to another robot, the network should be able to detect such a potentially risky situation and provide its UE with highly reliable connectivity, in order to enable a much more accurate automated remote control of the machine or a complete stop, if necessary. The security and safety procedures put in place under these circumstances typically demand very strict communication reliability levels, e.g. such that the packet loss probability is kept between 10^{-5} and 10^{-9}, according to standard specifications [21]. This requirement goes beyond the 5G URLLC capabilities, that is expected to deliver a reliability of up to 10^{-5}. A dangerous proximity situation is identified when the detected distance between two UEs reaches or becomes smaller than a given value r called *critical distance*. On the contrary, when the two UEs are distant more than r, then the reliability requirements of the robot control communication channel are less stringent and can be relaxed, e.g. to tolerate a packet loss probability of 10^{-2}.

As already mentioned, dynamically adapting the communication reliability level to the current distance between two UEs implies changing the amount of redundant channels connecting those UE to the core network. This is a feature that is not available yet in current 5G network deployments, which can at best provide dual connectivity for URLLC services in a static manner, often not being sufficient to enforce the required high reliability levels [7]. Rethinking the role of some of the components of the core network could bring to solutions that enforce dynamic reliability only when needed, thus saving resources and reducing energy consumption while guaranteeing the required safety conditions [9].

In line with our previous studies, we consider an evolved hierarchical control plane architecture including multiple distributed components and a centralized one [10]. Distributed components are in charge of telemetry data collection and pre-processing to enforce fast, near real-time and system-specific control actions. The centralized component instead collects (possibly pre-processed) data from multiple distributed components so that it can take advantage of a broader view of the status of the overall system and make more informed decisions on the definition and refinement of the policies operated by the distributed components.

More specifically, a relevant set of tasks to be performed by the control plane includes:

- keeping track of the moving UEs and their relative distance, to detect when they reach the critical value r;
- monitoring the quality of the communication channels accessible to each UE, to determine the reliability level currently provided to the UE;
- in case a given UE pair is within critical distance, identifying a suitable combination of redundant communication channels to be maintained or established for each UE, to provide the required high reliability level;
- in case a given UE is not within critical distance with any other UE anymore, tearing down any redundant communication channel to save in terms of resource usage and energy consumption.

The execution of the tasks mentioned above would significantly benefit from a distributed implementation approach, as proved in our previous work [9], [10], representing thus an interesting use case for the hierarchical control plane architecture considered in this paper. In particular, instead of having a single, centralized control plane entity in charge of monitoring the whole industrial area deciding on the best combination of redundant channels, we assume that the industrial area is split into a number of sub-areas, as shown in Fig. 1. Each sub-area is managed by a dedicated distributed element that works on a subset of resources (e.g., the UEs, their positions, and the available communication channels within the respective sub-area), thus allowing faster execution times of the redundant communication channel allocation algorithm.

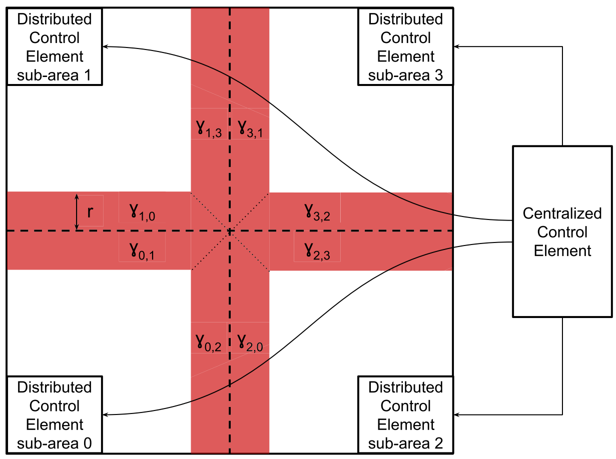

FIGURE 1. Representation of a factory floor split into four sub-areas (dashed black lines). Each sub-area includes its own "Distributed Control Element," controlled by the "Centralized Control Element," and a number of UEs and ANs (not shown). The zone within distance r from the borders is highlighted in red, where the border policy coefficients $\gamma_{i,j}$ are represented.

As reported in detail in our previous work [10], the objective of the algorithm is to minimize the number of communication resources employed while satisfying the reliability constraint on the overall packet loss rate. To do so, for each UE in every sub-area, the relevant distributed component orders the ANs based on the coverage they offer to the UE, then selects the first one and checks whether the UE would meet its target reliability requirement with only a connection to that AN. The process continues until either a suitable set of connections is found, or no set of connections allows to satisfy the requirement. While each distributed component is in charge of finding the solution to this problem within the respective sub-area, the centralized element determines how many sub-areas the whole scenario should be divided into, the reliability levels required in each sub-area, and the set of *border policies* to be enforced between adjacent sub-areas. Border policies are needed because some UEs could be located within critical distance r from the respective sub-area borders, i.e., within the red zones depicted in Fig. 1. Each distributed component is aware of the position of the UEs located inside its assigned sub-area only, so it cannot determine whether a UE that is located very close to the border is within critical distance from another UE in a neighboring sub-area.

For this reason, the centralized component may enforce a policy to manage these situations, for instance by defining for each border between the adjacent sub-areas i and j a coefficient $\gamma_{i,j}$ that represents the probability of enforcing high reliability levels for UEs that are within critical distance from that border. Choosing $\gamma_{i,j} = 1$ means that a distributed component will apply a conservative policy, resulting in excessive resource consumption due to redundant communication channels always on, even when the UEs do not actually need them [9]. Conversely, with $\gamma_{i,j} = 0$ reduced resource consumption is expected, but such a loose policy might result in cases with insufficient reliability levels.

Further details on the algorithmic aspects of the system under study can be found in our previous work [7], [9], [10], and in the appendix of this paper. A discussion on how the current 5G core network could evolve to support the envisioned dynamic reliability feature is reported in Section IV.

B. DYNAMIC RELIABILITY BASED ON DISTANCE AND TASK AWARENESS

Considering the current state of the art in HRC as reported in Section II, we can add another condition to the enforcement of dynamic reliability, besides the concept of critical distance. We can indeed model each worker to be performing either a collaborative or an autonomous task, at any given time. There might also be instances when the worker is idle, waiting for the next task to start. In this state, it is not interacting with other workers, so we can consider idle states as being part of the autonomous tasks. Assuming that workers performing autonomous tasks are not subject to risky situations, even when they are distant from another worker less than the critical value r, then enforcing high reliability levels is not necessary under these circumstances.

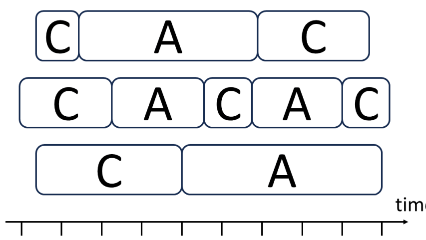

FIGURE 2. Example of the evolution of tasks of workers over time.

Specifically, at any given time a UE can be performing either a collaborative (C) or an autonomous (A) task. An example illustrating the evolution in time of working tasks is given in Fig. 2, with each horizontal sequence representing the task of a worker, and the ticks on the time axis representing the observation instants. By combining this observation with the information on the location of UEs, we can determine the reliability need of the UE at a given instant, by classifying it into either one of two categories, corresponding to the two defined reliability levels.

Overall, our approach to determine an appropriate set of communication channels for each UE to implement dynamic reliability is structured in two phases, namely a *classification* and an *assignment* phase, as represented in Fig. 3. In the *classification* phase, the inputs coming from the environment are analyzed, and the UEs are classified as either requiring high or low reliability levels. The rationale is that a UE should be granted a higher reliability if it is too close to at least another UE and it is performing collaborative tasks, or a lower reliability otherwise. Therefore, the first check is on relative

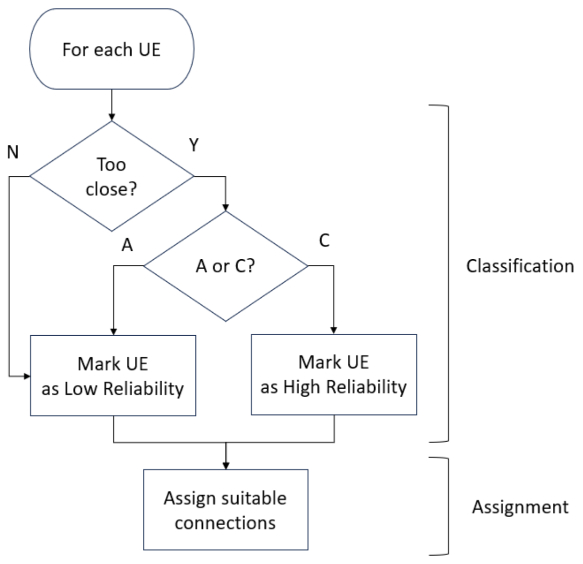

FIGURE 3. **Methodology for determining dynamic reliability levels based on distance and task awareness.**

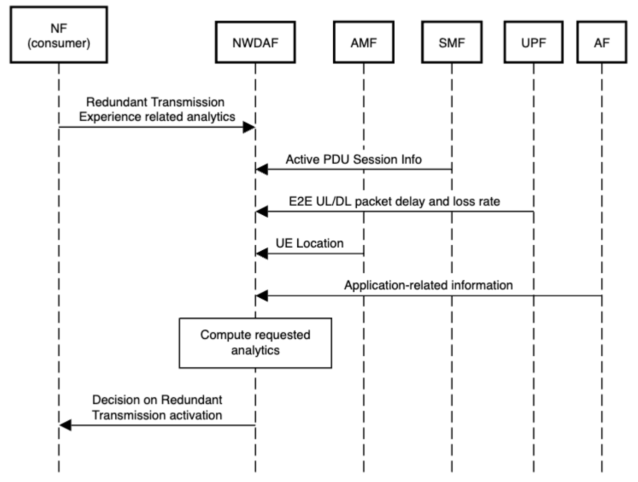

FIGURE 4. **Simplified diagram for the Redundant Transmission Experience analytics procedures (the complete version can be found in Fig. 6.13.4.1-1 of [22]).**

distance, using the information on location provided by the appropriate network function (e.g., from the 5G Location Management Function). If the distance of the considered UE from at least another UE is larger than the critical value r, then the UE is marked as requiring low reliability. Otherwise, the second check is on the task associated with the UE at the observed time: if it is a collaborative one, the UE is marked as requiring high reliability, or low otherwise. In the *assignment* phase, each UE is assigned either a single or an appropriately redundant set of communication channels based on its predetermined reliability requirement.

These phases are executed periodically, in correspondence to the observation time instants represented in Fig. 2. The period of execution of this process, inversely proportional to the frequency of such observations, depends on a number of factors, including specific safety requirements in the environment, which in turn depend on the application.

There might be times when the reliability requirement cannot be correctly enforced, either for scarcity of resources or unforeseen conditions. In such circumstances, an alarm might be issued, interrupting the activities of the involved workers until the reliability conditions are met again. As a practical example, when a human worker needs to interact with an industrial robot to manufacture an object and presses the button to open the glass panel separating them, the network might determine that there is a coverage problem, and the glass panel may not open until the network signals that the reliability conditions are met again. This additional safety measure is one of the ways in which the network can actively contribute to improving safety.

IV. EVOLUTION OF 5G CORE NETWORK TOWARD DYNAMIC RELIABILITY

Before delving into the performance analysis of the dynamic reliability feature, we believe it is essential to include some considerations on the actual feasibility of the proposed approach in the framework of the current 5G mobile network architecture and discuss about the gaps that might be addressed in its evolution toward 6G. As part of technical specification TS 23.288, 3GPP presents several applications of the Network Data Analytics Function (NWDAF), the 5G core network component in charge of managing the analytics on data coming from the network [22]. In detail, the NWDAF can subscribe to notification events coming from other core network functions, such as Session Management Function (SMF), Policy Control Function (PCF) and User Plane Function (UPF), and external applications, directly as Application Functions (AFs) or through the Network Exposure Function (NEF). Furthermore, the NWDAF can run algorithms that consume the collected data to produce analytics that can be distributed to other network functions, to help with their network management duties.

In TS 23.288, Section 6.13 presents the “Redundant Transmission Experience related analytics,” describing a mechanism in which the NWDAF gathers data from relevant network functions and informs the analytics subscribers (or consumers) on the predicted uplink/downlink packet drop rate over a given time slot, and whether the redundant transmission should be activated or not for that time slot. In this context, the consuming network functions can be either the PCF or the SMF, depending on the type of redundancy considered (see Sections 5.33.2.1 and 5.33.2.2 in technical specification TS 23.501 [23]). Fig. 4 depicts a simplified representation of this procedure. Once requested by a network function (e.g., the PCF or the SMF), the NWDAF starts collecting the relevant metrics to compute whether redundant transmission is needed over a given time slot. To accomplish this, the NWDAF receives from the SMF the current status of the active PDU session (e.g., the Data Network Name associated with the URLLC service) and from the AMF the position of the UE. Then, it acquires the measured end-to-end uplink/downlink delay and loss rate from the UPF. Finally,

TABLE 1. Values of simulation parameters for different considered scenarios.

	Scenario 1	Scenario 2	Scenario 3	Scenario 4	Scenario 5	Scenario 6	Scenario 7	Scenario 8	Scenario 9
Factory size [m^3]	$100 \times 100 \times 10$								
Critical distance [m]	3								
"Low" reliability	99%								
"High" reliability	99.999%								
Amount of sub-areas	1	2	6	1	1	2	2	1	2
Amount of ANs	25	36	64	25	25	36	36	36	36
Amount of UEs	10 (5+5)	20 (10+10)	120 (72+48)	40 (20+20)	100 (50+50)	50 (25+25)	100 (50+50)	120 (60+60)	120 (60+60)

the information related to the application status is obtained from the AF. After gathering all this data, the NWDAF can determine the Redundant Transmission Status over a given analytics target period and relay this choice to the consuming NF. The standard does not specify the exact algorithm the NWDAF should adopt to compute these analytics.

As described above, within this procedure, 3GPP has already standardized that the NWDAF can receive event notifications to influence the PDU status from external applications through the *Naf_EventExposure_Subscribe* service. However, the current version of the standard supports only a limited set of event types, none of which are directly related to industrial applications [24]. Nonetheless, we believe the information related to the industrial application under study (e.g., the type of task) could be included in the *SVC_EXPERIENCE* event type, while we hope for more fine-grained support of event type in the future mobile generation. Furthermore, in this version of the standard, the NWDAF only returns a boolean value for the Redundant Transmission Status, while to enable our approach, it should also communicate the number of and which active redundant paths are needed to meet the service requirements.

The actual capability of 5G networks to dynamically switch between redundant and non-redundant data plane connections is still under study. Yet, we expect that 6G will allow greater connection flexibility to improve the overall energy efficiency. Furthermore, the support of multi-connectivity in 6G is foreseen by projects like Hexa-X-II to support the increase in the reliability requirements of future services [25].

V. PERFORMANCE ANALYSIS AND RESOURCE GAIN

This section includes detailed results of a simulation campaign that we carried out to assess dynamic reliability performance and resource gain. The reference scenario considers a square factory floor of $100\,\text{m} \times 100\,\text{m} \times 10\,\text{m}$, with ANs deployed on a regular grid, and UEs moving randomly over the floor. The factory floor might be divided into sub-areas, each encompassing a portion of the available coverage resources. The critical distance between UEs is set to $r = 3\,\text{m}$, and UEs within that distance from each other are considered to be under critical safety conditions, or non-critical otherwise. The reliability level requirements are 99% under non-critical conditions (*low reliability*) and 99.999% under critical conditions (*high reliability*). All simulation parameters are summarized in Table 1.

The following results show that by applying dynamic reliability by means of dynamic assignment of redundant communication channels to UEs, we can achieve complete satisfaction (i.e., allocate to each UE a sufficient number of channels so as to satisfy its distance-dependent reliability requirements) by using a smaller number of resources compared to static assignment (i.e., allocate to each UE a pre-determined amount of channels between 1 and 2, as in the current 5G standard).

We start by running simulations to assess the amount of communication resources necessary to satisfy all the users in the scenario, with different amounts of sub-areas, active UEs, and deployed ANs. For this assessment, we consider Scenarios 1 to 9, as described in Table 1. We represent the results of Scenario 1 in Fig. 5, and provide the other results numerically in Table 2. Connections are selected according to the approach mentioned in Section III-A.

To fulfill the target reliability levels within a single sub-area (i.e., without splitting the factory floor) and 10 UEs in total (5 humans and 5 robots), we need at least 25 ANs. The results in Fig. 5a show that, with static assignment of connections, all UEs in non-critical conditions (i.e., requiring low reliability) are always satisfied allocating only one communication channel. However, in order to satisfy UEs in critical conditions, in many instances more than two channels are necessary, as shown by the fact that with dual static connectivity only a portion of UEs in critical conditions are satisfied. With dynamic *multi*-channel assignment, all UEs in all conditions are satisfied.

The results in Fig. 5b complement these observations, by showing that under such coverage conditions, almost all UEs can be satisfied with only a single channel, making the dual static connectivity scheme an inefficient waste of resources, but also showing that in some cases it is important to be able to cope with more demanding requirements, i.e., more than two channels per UE, in order to guarantee full satisfaction to all users. Specifically, under these coverage conditions some UEs need up to 5 channels in order to meet their reliability requirements, as shown by the cumulative distribution curve extending to the value of 5. The gain in terms of communication resource usage achieved by adopting

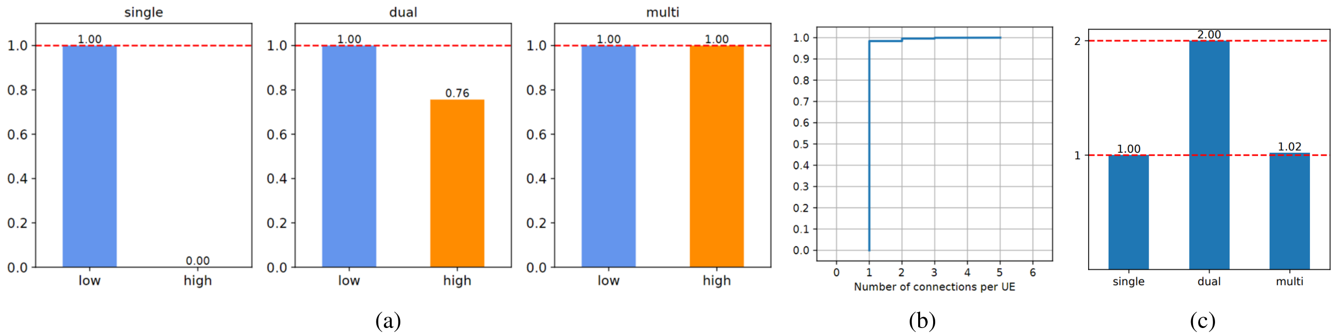

FIGURE 5. Performance indicators for Scenario 1 (with 1 sub-area, 25 ANs, 10 UEs). (a) Fraction of UEs that achieved target reliability (low: 99%, high: 99.999%) comparing single and dual static connectivity versus multiple dynamic connectivity. (b) Cumulative distribution of the number of channels per UE that achieved target reliability. (c) Resource consumption comparing single and dual static connectivity versus the average number of channels under multiple dynamic connectivity.

TABLE 2. Performance indicators for Scenarios 1 to 9, as described for Fig. 5.

	Static connectivity		Dynamic connectivity				
	Fraction of UEs achieving high reliability with		Fraction of UEs achieving target reliability with			Connections per UE (avg.)	Connections per UE (max)
	1 connection	2 connections	1 connection	2 connections	3+ connects.		
Scenario 1	0.00	0.76	0.97	0.98	1.00	1.02	5
Scenario 2	0.02	0.87	0.95	0.98	1.00	1.04	5
Scenario 3	0.03	0.96	0.83	0.98	1.00	1.17	4
Scenario 4	0.01	0.77	0.91	0.97	1.00	1.12	6
Scenario 5	0.01	0.75	0.81	0.95	1.00	1.24	6
Scenario 6	0.02	0.87	0.91	0.98	1.00	1.10	4
Scenario 7	0.02	0.88	0.82	0.97	1.00	1.19	5
Scenario 8	0.02	0.92	0.82	0.97	1.00	1.20	4
Scenario 9	0.02	0.88	0.82	0.97	1.00	1.24	5

the dynamic reliability feature is quantified in Fig. 5c, showing how the average resource consumption obtained with the dynamic multi-channel allocation scheme is only slightly larger than the single connectivity case. Therefore, under the considered conditions the use of dynamic reliability allows to always achieve the required safety levels, while keeping resource usage close to the minimum.

The first part of Table 2 is dedicated to the static assignment of connections, as in Fig. 5a, showing only the fraction of UEs that achieve high reliability with 1 or 2 connections. The results show that, even with 2 connections, high reliability cannot be provided to all UEs. Let us now focus on the dynamic connectivity in the right part of the table. We first consider a larger scenario than Scenario 1, already described in Fig. 5, with two sub-areas and 20 UEs in total (10 humans and 10 robots), where to fulfill the target reliability levels we need at least 36 ANs. Under these conditions, similar considerations to the previous scenario can be made, taking into account that the baseline static connectivity is slightly improved now due to the higher density of ANs. For an even larger scenario with 6 sub-areas and 120 UEs in total (72 humans and 48 robots), we need at least 64 ANs to be able to fulfill the target reliability levels. Under these conditions, the baseline static connectivity is now very competitive, yet still not able to satisfy all UEs reliability requirements at all times, and in any case still using the communication resources less efficiently than in the dynamic reliability case.

After assessing these baseline cases, we modify one parameter at a time to assess its impact on the overall performance. To begin with, we fix the number of sub-areas to one and the number of ANs to 25, and we change the number of UEs from 40 to 100. By increasing the number of UEs the number of channels per UE needed to achieve the required reliability levels also increases, as more critical situations arise. This can be observed from the fact that fewer UEs are satisfied with a single channel, with an increasing part of them requiring two or more channels to meet their reliability requirements. Similar observations can be made for the case of two sub-areas with 36 ANs, considering either 50 or 100 UEs.

Then, we fix the number of UEs to 120 and the number of ANs to 36, and we consider either one or two sub-areas. The results show that the performance and resource gain is basically identical, although splitting the factory floor in sub-areas gives a tangible advantage in terms of algorithm execution time, as previously reported in [9].

VI. PERFORMANCE OF TASK AWARENESS

To assess the impact of task awareness on the performance of dynamic reliability, we extended our simulation tool to include the classification criteria described in Section III-B.

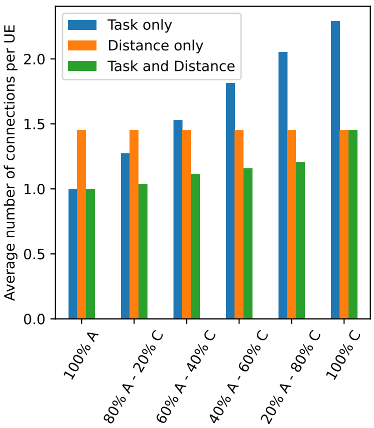

FIGURE 6. **Impact of different classification inputs on communication resource usage, when applying dynamic reliability.**

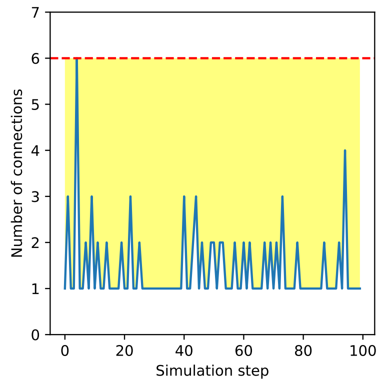

FIGURE 7. **Evolution over time of the channels of a single UE, when dynamic reliability is enforced.**

Where not otherwise specified, we consider a scenario with 1 sub-area, 25 ANs, and 120 UEs, similar to those considered in Section V.

As a first evaluation, we want to assess the impact of task-based classification on the usage of communication resources, and compare it with that of distance-based classification alone, as well as with the combined effects of the two criteria. In order to isolate the effect of task-based classification, we temporarily exclude the check on distance, by setting the critical value to $r = 0$. This way, according to the rationale of the classification phase explained in Section III-B, the UEs will be classified as requiring high reliability as often as they execute collaborative tasks. Vice versa, to apply distance-based classification only, we set the critical distance to $r = 3$ m, and force the UEs in a collaborative state at all times, resulting in them being classified as requiring high reliability as soon as they are closer than the critical distance value. To consider both effects, we apply the full procedure depicted in Fig. 3.

In Fig. 6, the bars depict the average number of connections assigned to a UE, for a range of task distributions. Different series of bars represent different criteria for the classification. On the left end of the horizontal axis we denote the case where all UEs are carrying out autonomous tasks at all times. There, when tasks are considered (either alone or combined with distance), none of the UEs requires multiple channels in the simulated coverage conditions as the safety conditions are still met with low reliability, resulting in all of them being satisfied with only one channel. Conversely, on the right end of the same axis we have the case where all UEs are always carrying out collaborative tasks. In that case, if the reliability level is chosen solely based on tasks and the information on the relative position of UEs is ignored (*Task only*), all UEs will require high reliability at all times. This, in turn, causes all UEs to require multiple channels, resulting in a less effective resource usage. In the same case, if distance is considered in the classification (*Task and Distance*), the performance remains independent of the inclusion of (always collaborative) tasks, in line with the rationale used for classifying UEs. In fact, in this case, such performance is the same as when considering the relative distance between UEs only (*Distance only*). The intermediate cases represent different distributions of activities, with varying probabilities of a UE performing a collaborative or an autonomous task. Overall, we can observe that by considering both tasks and distance in determining the appropriate level of dynamic reliability, the system utilizes the lowest average number of channels, outperforming the cases where only one of these inputs is taken into account.

We can also remark that, even when the average number of channels per UE is at its highest, it is still lower than the total number of channels that would be necessary to provide the same coverage to UEs in a static scenario, i.e., giving the same number of channels to each UE at all times. For example, when the average value is slightly larger than 2, the static number of channels to be provided to guarantee complete satisfaction would be at least 3, or up to 6 considering some worst-case situations (such as the one depicted in Fig. 7), when there are likely many UEs that would be satisfied with fewer channels than that.

A representation of the number of channels assigned to a single UE over the simulated time span is shown in Fig. 7. This figure refers to the case where both tasks and distance are considered in the classification, and all UEs perform collaborative tasks for 60% of the time (i.e., the *40% A - 60% C* case in Fig. 6). This value was picked because it was derived from the distribution of tasks represented in a real-world use case [12]. The horizontal red line at the top represents the worst possible case of required static connections to cover the UE ensuring the appropriate reliability at all times, given by the maximum number of channels that the UE required in the simulation run. This supports the claim (already proven in [7], [9]) that in certain conditions the dual connectivity approach of 5G is not enough to guarantee the required reliability, even when taking into account the tasks that the UEs are performing. The area highlighted in yellow represents the amount of communication resources that can be spared by employing a

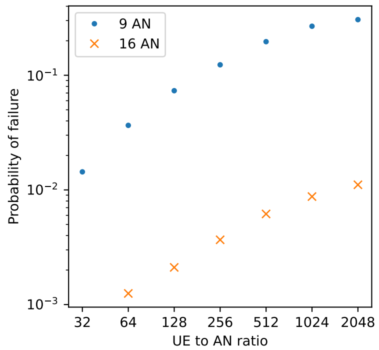

FIGURE 8. **Probability of failure in enforcing the required reliability.**

dynamic approach to reliability rather than a static coverage that needs to guarantee high reliability at all times.

We can observe that the channels assigned to this UE vary from 1 to 6, depending on the reliability requirements. In fact, based on this observation, if the coverage of the area were to be made statically and thus had to always meet the high reliability requirement, the UE would need to be assigned up to 6 channels constantly, while with a dynamic approach, up to 5 channels per assignment could be spared. Even if we were to neglect the values higher than 3 in Fig. 7, the dynamic approach would still allow for significant resource saving.

We also tackle the issue of how to dimension the system, i.e., how many communication resources are needed to guarantee a certain level of reliability and preserve the workflow when task awareness is taken into account. According to the rationale suggested in Section III-B, when the network determines that it cannot guarantee the required reliability level, we suggest it may issue an alarm to prevent other safety measures to unlock and enable the collaboration between human and robot workers. This preserves the safety of the workers, although it impacts the workflow. In Fig. 8 we represent how the lack of sufficient resources might impact the activities, by plotting the probability of having at least one failure in enforcing the reliability level associated with a UE as a function of the ratio between the number of UEs and ANs assumed in the scenario, for different numbers of ANs. For this evaluation, we still refer to the *40% A - 60% C* case of Fig. 6. We can observe that, even for a rather scarcely covered scenario as the one with 16 ANs over the whole area, a tangible quantity of failures starts to arise only when the UEs outnumber the ANs 64-to-1.

VII. EVALUATION OF NETWORK SIGNALING OVERHEAD INDUCED BY DYNAMIC RELIABILITY

In the framework of the dynamic reliability approach under investigation, a critical aspect to be considered is to ensure timely and reliable data collection to guarantee the correctness of the decision making process. More specifically, with reference to the HRC use case, ultra-reliable communications must be enforced to guarantee that the relative position of humans and robots – by means of the UE they carry – is correctly detected by the robot control system, especially when the distance between them is under the critical value r.

Obviously, more frequent updates of the human and robot positions result in a more accurate detection and a stricter enforcement of the safety requirements, with upper bounds imposed by technology constraints, such as the accuracy of the position detection system adopted, or the time required to process the incoming data and enforce any decision made by the control system. However, frequent updates of the UE positions may cause additional overhead in the signalling system, which is to be factored in in terms of a cost component, or overhead, of the dynamic reliability approach. What follows includes some initial considerations on how to quantify such an overhead and how it depends on system variables. The list of symbols we use and their meaning is reported in Table 3.

TABLE 3. **Definitions of symbols used in the evaluation of signalling overhead.**

Symbol	Definition
α_i	Angle associated with UE_i movement, $i \in \{1, 2\}$
d_i	Distance $d(t)$ between the two UEs at time t_i
f	Frequency of data collection
l_i	Distance traveled by UE_i, $i \in \{1, 2\}$
r	Critical distance, i.e., the distance at which the enforcement of high reliability is triggered
d_0	Value of the distance $d(t)$ between the two UEs under which the network must already be enforcing high reliability
r_{min}	Minimum value of the critical distance that allows high reliability to be enforced at distance d_0
T	Time between any two subsequent detection times t_{i-1},t_i
t_e	Time needed to enforce the required reliability in the network
v_i	Speed of UE_i, $i \in \{1, 2\}$

A. DETERMINING THE DATA COLLECTION FREQUENCY

To start tackling the problem, we make the following simplifying assumptions:

1) we consider two UEs only, namely UE_1 and UE_2;
2) the two UEs move within an open space without obstacles;
3) the positions of the two UEs are periodically detected at some given time instants t_i, with period $t_i - t_{i-1} = T, \ \forall i = 1, 2, \ldots$;
4) the two UEs move with constant speeds, respectively v_1 and v_2;
5) the distance between the two UEs as a function of time is given by $d(t)$;
6) between any two subsequent detection times t_{i-1} and t_i, the UEs move along a straight trajectory, but the direction can change in each interval, as illustrated in Fig. 9;
7) at any time instant t_i, the angles between the moving direction and the straight line connecting the two UEs are $\alpha_{1,i}$ and $\alpha_{2,i}$, respectively;
8) we consider only the case when both $\alpha_{1,i}$ and $\alpha_{2,i}$ are between 0 and 90°.

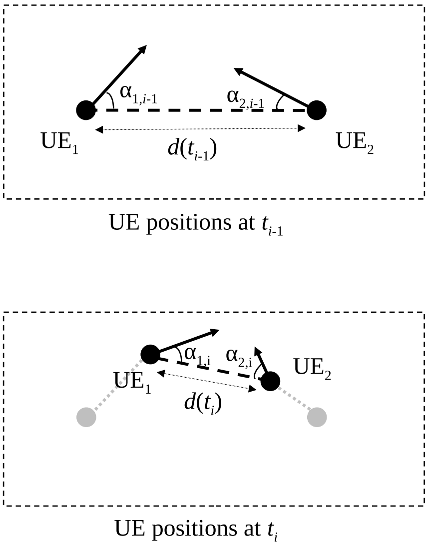

FIGURE 9. UE positions and relative distance at detection times t_{i-1} and t_i.

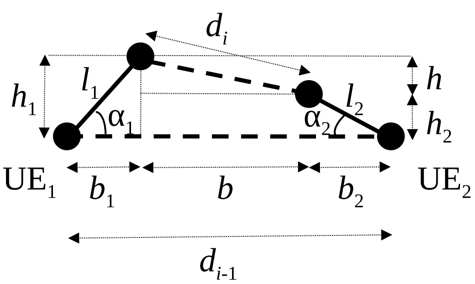

FIGURE 10. Geometric representation of the relation between d_i and d_{i-1}.

Under the previous assumptions, and defining $d_i = d(t_i)\ \forall i$, the distance between the two UEs at time t_i can be computed knowing the distance at time t_{i-1} as illustrated in Fig. 10. In the interval (t_{i-1}, t_i) the distances covered by the two UEs are, respectively:

$$l_1 = v_1 T \quad \text{and} \quad l_2 = v_2 T.$$

From Fig. 10, knowing that:

$$\begin{aligned} h_1 &= l_1 \sin\alpha_1 \quad b_1 = l_1 \cos\alpha_1 \\ h_2 &= l_2 \sin\alpha_2 \quad b_2 = l_2 \cos\alpha_2 \\ b &= d_{i-1} - (b_1 + b_2) \quad h = h_1 - h_2 \end{aligned}$$

we can write:

$$\begin{aligned} d_i &= \sqrt{b^2 + h^2} = \\ &= \sqrt{(d_{i-1} - (b_1 + b_2))^2 + (h_1 - h_2)^2} = \\ &= \Big[(d_{i-1} - (l_1 \cos\alpha_1 + l_2 \cos\alpha_2))^2 + \\ &\quad + (l_1 \sin\alpha_1 - l_2 \sin\alpha_2)^2\Big]^{1/2} = \\ &= \Big[(d_{i-1} - (v_1 \cos\alpha_1 + v_2 \cos\alpha_2)\, T)^2 + \\ &\quad + (v_1 \sin\alpha_1 - v_2 \sin\alpha_2)^2\ T^2\Big]^{1/2}. \end{aligned}$$

In the particular case when the two UEs are directed toward each other along a straight trajectory, which is also the case when they are approaching to each other at maximum speed, we have $\alpha_1 = \alpha_2 = 0$ and:

$$d_i = d_{i-1} - (l_1 + l_2) = d_{i-1} - (v_1 + v_2)\, T. \tag{1}$$

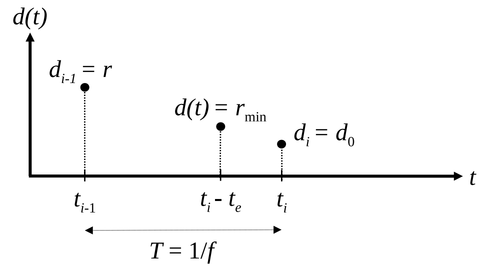

FIGURE 11. Time diagram showing the evolution of $d(t)$ and the role of other parameters.

Knowing the relation between d_i and d_{i-1}, we can obtain the value of the critical distance r that triggers the enforcement of high reliability as a function of the frequency of data collection $f = 1/T$. Let us refer to the time diagram shown in Fig. 11. Defining t_e as the time needed to process incoming data and enforce the required reliability in the network, two subsequent detection instants t_{i-1} and t_i must be separated by at least a period of time equal to t_e. Therefore, an upper bound on f is given by:

$$f \leq \frac{1}{t_e}.$$

Denoting with d_0 the value of the distance between the two UEs under which the network must already be enforcing the high reliability level, the minimum value of the critical distance $r_{\min}$ that must trigger the enforcement of high reliability must be the value of the distance measured at an interval t_e before the instant the two UEs reach distance d_0. From equation (1), when $\alpha_1 = \alpha_2 = 0$, this condition is met when:

$$d_0 = r_{\min} - (v_1 + v_2)\, t_e$$

from which we can write:

$$r_{\min} = d_0 + (v_1 + v_2)\, t_e.$$

In general, the value of the critical distance r as a function of the frequency of data collection is:

$$r = d_0 + \frac{(v_1 + v_2)}{f} \geq r_{\min}. \tag{2}$$

Alternatively, we can determine the data collection frequency as a function of the critical distance r and the speed of the UEs, again when $\alpha_1 = \alpha_2 = 0$, as:

$$f = \frac{v_1 + v_2}{r - d_0}. \tag{3}$$

Due to the assumption on the angles $\alpha_1 = \alpha_2 = 0$, the frequency only depends on the sum of the speeds of the two UEs. This assumption is conservative, as this situation represents the "worst case scenario", i.e., when the distance that the two UEs need to travel before high reliability needs to be enforced is minimum. This also simplifies the overall positioning-based system as there is no need to know or predict the trajectories/angles of the UEs.

B. AN ILLUSTRATIVE EXAMPLE

To better understand the use of (2) and (3), let us consider the example reported in Fig. 12. A robot and a human are moving toward each other along a straight path with speeds v_1 and v_2, respectively. d_0 is the distance at which, due to strict safety requirements, the high reliability must already be in place and is represented by a red circle in Fig. 12. Since it takes some time t_e to process UE positions and reconfigure the network resources, e.g., when changing from low to high reliability levels, the reconfiguration must start at a distance $r > d_0$. This distance is what we call *critical distance*.

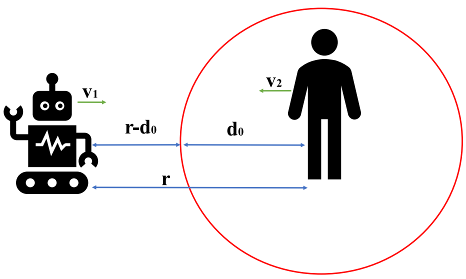

FIGURE 12. Illustrative example of the definition of critical distance.

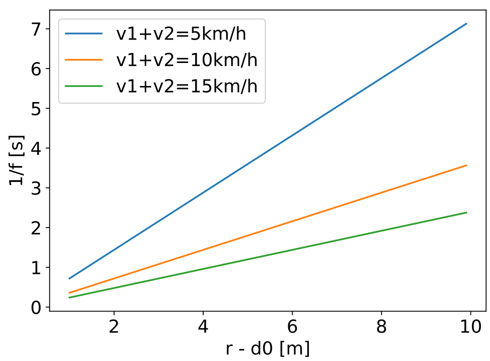

FIGURE 13. Maximum period between two consequent positioning samples ($T = 1/f$) as a function of the difference between the critical distance and the distance at which the high reliability must already be in place ($r - d_0$), for three different values of the sum of speeds of robot UE_1 (v_1) and human UE_2 (v_2).

Fig. 13 reports the time between two consecutive positioning samples (i.e., the period $T = 1/f$ at which the samples must be collected) as a function of the critical distance margin $r - d_0$, for different values of the sum of the UE speeds $(v_1 + v_2)$. For example, if we set $r - d_0$ to 6 m and the sum of the speeds is 5 km/h, the system needs to collect the UE positions every 4.3 s. If the sum of the speeds is 10 km/h or 15 km/h, the position needs to be collected more frequently, i.e., every 2.1 s and 1.4 s, respectively. Equation (3) then represents a possible way to quantify the network signalling overhead induced by the dynamic reliability feature.

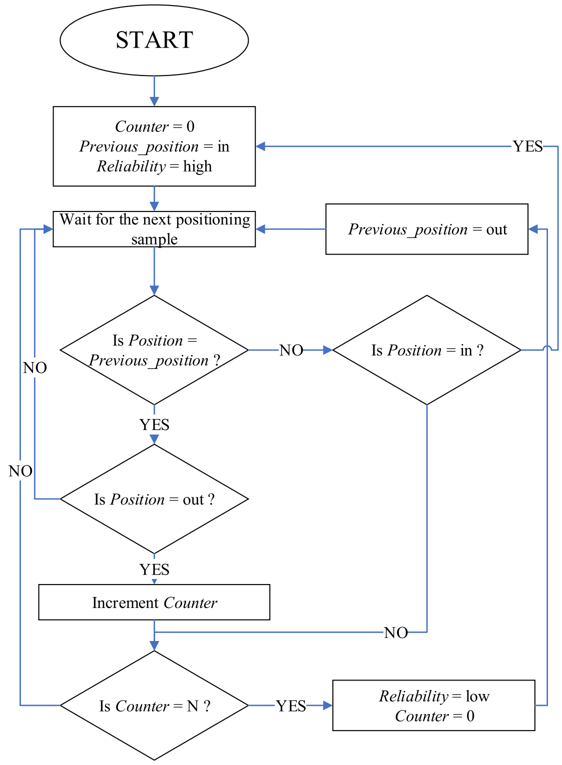

FIGURE 14. Flowchart of a possible algorithm to limit frequent reconfigurations between high and low reliability levels.

C. LIMITING FREQUENT NETWORK RECONFIGURATIONS

The proposed mechanism checks if the distance between the two UEs is larger or smaller than r. It is possible to define a region around UE_1 given by r. As soon as UE_2 moves inside this region, the transition from low to high reliability must be started. This is required to have the high reliability enforced at the time UE_2 is distant d_0 from UE_1. On the other hand, when UE_2 is moving away from UE_1 and their distance becomes larger than r, the transition to low reliability is triggered. This might lead to frequent network reconfigurations between high and low reliability, especially in the case when the two UEs are working at a distance close to r from each other. To reduce the number of reconfigurations, the transition between high and low reliability can be delayed. After N consecutive samples in which the two UEs are at a distance larger than r, the reconfiguration is triggered. The transition from low to high reliability instead is immediately triggered when the distance between the two UEs is less than r, for safety reasons. The flowchart of this strategy is reported in Fig. 14. It relies on the following variables:

- *Counter*, used to count up to N samples;
- *Previous_position*, that tells if the two UEs were inside (in) or outside (out) the region defined by r at the previous sample detection time;
- *Reliability*, used to store and change the reliability level (either *high* or *low*);
- *Position*, that tells if the two UEs are inside (in) or outside (out) the region defined by r, based on the current sample detection time.

Each time the *Reliability* value changes, the system must trigger the corresponding change in the network configuration. It should be noted that there is a trade-off between the number of reconfigurations and the size of the interval during which the two UEs are connected with high reliability. In fact, reducing the former increases the value of the latter, and consequently the use of resources.

VIII. CONCLUSION

In this paper, we have addressed the issue of improving safety in industrial environments, where humans and robots cooperate, by leveraging the help that the network can offer. In fact, in modern industrial scenarios where all workers carry a mobile device connected to the indoor access network, the reliability of the connection can be controlled dynamically, to make sure that emergency commands are received timely, when needed. This control can be based on multiple inputs, including the distance between connected devices, and the type of task the worker associated with the device is carrying out. With this paper we significantly extended our previous work on dynamic reliability by evaluating performance, resource gain and costs of the approach, and by exploring how to leverage the knowledge of the specific nature of the tasks being performed by robots collaborating with humans.

The results of our study demonstrated that applying dynamic reliability can support hyper reliability requirements and lead to significant savings in terms of communication resource consumption compared to the static redundancy solutions offered by current 5G deployments, and that the cost in terms of network signalling overhead can be limited to an acceptable level. The novel concept of task-aware dynamic reliability adds a new dimension to the efficient deployment of HRLLC services in future 6G networks by taking advantage of some of the peculiarities of a given vertical application. Overall, the results of our study show that the dynamic reliability technology can overcome the limitations of 5G URLLC communications and meet the capabilities expected in 6G systems to support HRLLC type of communications in industrial scenarios. The final objective is to have the network assist the operations within industrial environments and make the workplace safer, while also efficiently use communications resources and reduce the cost.

APPENDIX
RESOURCE ASSIGNMENT ALGORITHM FOR DYNAMIC CONNECTIVITY

For completeness, we reproduce the algorithm introduced in [9], which handles the dynamic allocation of connectivity resources. The assignment of dynamic connections is performed in two distinct phases. The classification phase identifies UEs in critical conditions based on their mutual distances and, optionally, the nature of the tasks they are executing. This is followed by the decision phase, during which the resource assignment algorithm is applied. Table 4 summarizes the symbols used throughout the algorithm. Algorithm 1 presents the logic behind the selection of connectivity resources, focusing on the decision phase. The classification phase is assumed to be executed beforehand, resulting in a set C of UEs identified as being in critical conditions. The core idea of the algorithm is to iteratively explore combinations of available connections for each UE. These connections are first ranked in order of increasing loss rate. The algorithm then evaluates subsets of the top-ranked connections, starting from the single best one, then the top two, and so on, until it finds a combination that satisfies the predefined loss rate requirement.

TABLE 4. System and performance variables.

List of Variables	
U	Set of User Equipments (UEs), $\lvert U\rvert = N_U$
A	Set of Access Nodes (ANs), $\lvert A\rvert = N_A$
$A_i \subseteq A$	Set of ANs available to UE u_i
$\bar{b}_U$	Max number of connections (bearers) per UE
$\bar{b}_A$	Max number of connections per AN
b_i	Number of active connections of UE u_i
b_j	Number of active connections of AN a_j
$\mathcal{B}_i$	Candidate connection set for UE u_i
ℓ_d	Maximum acceptable (target) loss rate
C	Set of UEs in critical condition (connectivity risk)

Algorithm 1 Resource Assignment for Dynamic Connectivity

Require: Set of critical UEs C; max acceptable loss rate ℓ_d; max connections $\bar{b}_U$ per UE and $\bar{b}_A$ per AN
  for all $u_c \in C$ **do**
    Initialize assigned connection set: $\mathcal{B}_c \leftarrow \emptyset$
    Compute individual loss rate ℓ_j using a single connection b_j for each available AN $a_j \in A_c$
    Construct ordered list $\mathcal{B}_{\text{sorted}} = \{b_1, b_2, \dots, b_{|A_c|}\}$ by increasing ℓ_j
    $k \leftarrow 1$
    while $\mathcal{B}_c = \emptyset$ **and** $k \leq \min(\bar{b}_U, \bar{b}_A)$ **do**
      Let $\mathcal{B}_c^{(k)} \leftarrow \{b_1, \dots, b_k\}$
      Estimate combined loss rate ℓ_k for set $\mathcal{B}_c^{(k)}$
      if $\ell_k \leq \ell_d$ **then**
        $\mathcal{B}_c \leftarrow \mathcal{B}_c^{(k)}$
        break
      end if
      $k \leftarrow k + 1$
    end while
    Store final assignment $\mathcal{B}_c$ for UE u_c
  end for

REFERENCES

[1] W. Xian, K. Yu, F. Han, L. Fang, D. He, and Q.-L. Han, "Advanced manufacturing in industry 5.0: A survey of key enabling technologies and future trends," *IEEE Trans. Ind. Informat.*, vol. 20, no. 2, pp. 1055–1068, Feb. 2024.

[2] R. Bolla, R. Bruschi, F. Davoli, C. Lombardo, A. Mohammadpour, R. Trivisonno, and W. Y. Poe, "Adaptive reliability for the automated control of human–robot collaboration in beyond-5G networks," *IEEE Trans. Netw. Service Manage.*, vol. 20, no. 3, pp. 2489–2503, Sep. 2023.

[3] "Framework and overall objectives of the future development of IMT for 2030 and beyond," Int. Telecommun. Union, Radiocommunication Sector (ITU-R), Geneva, Switzerland, Tech. Rep. ITU-R M.2160-0, Nov. 2023. [Online]. Available: https://www.itu.int/rec/R-REC-M.2160-0-202311-I/en

[4] *Future Technology Trends of Terrestrial International Mobile Telecommunications Systems Towards 2030 and Beyond*. Accessed: Apr. 28, 2025. [Online]. Available: https://www.itu.int/pub/R-REP-M.2516

[5] G. Pocovi, H. Shariatmadari, G. Berardinelli, K. Pedersen, J. Steiner, and Z. Li, "Achieving ultra-reliable low-latency communications: Challenges and envisioned system enhancements," *IEEE Netw.*, vol. 32, no. 2, pp. 8–15, Mar. 2018.

[6] J. Rao and S. Vrzic, "Packet duplication for URLLC in 5G: Architectural enhancements and performance analysis," *IEEE Netw.*, vol. 32, no. 2, pp. 32–40, Mar. 2018.

[7] D. Borsatti, G. Davoli, C. Lombardo, D. Selvi, R. Bruschi, W. Cerroni, F. Davoli, C. Raffaelli, R. Trivisonno, and R. Bolla, "Adaptive network reliability for human–robot interaction in beyond 5G industrial applications," in *Proc. 18th Int. Conf. Design Reliable Commun. Netw. (DRCN)*, Mar. 2022, pp. 1–6.

[8] *Target Reliability Level Selection for Dynamic Reliability Configuration in a Network Slice*. Accessed: Apr. 28, 2025. [Online]. Available: https://patents.google.com/patent/WO2024146687A1

[9] D. Borsatti, G. Davoli, W. Cerroni, C. Raffaelli, W. Y. Poe, R. Trivisonno, and R. Bolla, "Distributed management of dynamic reliability in beyond 5G industrial environments for extreme low latency communication," in *Proc. 19th Int. Conf. Design Reliable Commun. Netw. (DRCN)*, Apr. 2023, pp. 1–7.

[10] D. Borsatti, G. Davoli, F. Tonini, W. Cerroni, C. Raffaelli, W. Y. Poe, and R. Trivisonno, "Hierarchical management algorithms for highly reliable communication in 6G industrial environments," *IEEE Netw. Lett.*, vol. 6, no. 1, pp. 36–40, Mar. 2024.

[11] *International Federation of Robotics*. Accessed: Apr. 28, 2025. [Online]. Available: https://ifr.org/

[12] A. Casalino, F. Cividini, A. M. Zanchettin, L. Piroddi, and P. Rocco, "Human–robot collaborative assembly: A use-case application," *IFAC-PapersOnLine*, vol. 51, no. 11, pp. 194–199, 2018.

[13] D. Mukherjee, K. Gupta, L. H. Chang, and H. Najjaran, "A survey of robot learning strategies for human–robot collaboration in industrial settings," *Robot. Computer-Integrated Manuf.*, vol. 73, Feb. 2022, Art. no. 102231.

[14] L. Gualtieri, E. Rauch, and R. Vidoni, "Development and validation of guidelines for safety in human–robot collaborative assembly systems," *Comput. Ind. Eng.*, vol. 163, Jan. 2022, Art. no. 107801.

[15] Y. Ghildiyal, R. Singh, A. Alkhayyat, A. Gehlot, P. Malik, R. Sharma, S. V. Akram, and L. M. Alkwai, "An imperative role of 6G communication with perspective of industry 4.0: Challenges and research directions," *Sustain. Energy Technol. Assessments*, vol. 56, Mar. 2023, Art. no. 103047. [Online]. Available: https://www.sciencedirect.com/science/article/pii/S2213138823000395

[16] C. Serôdio, J. Cunha, G. Candela, S. Rodriguez, X. R. Sousa, and F. Branco, "The 6G ecosystem as support for IoE and private networks: Vision, requirements, and challenges," *Future Internet*, vol. 15, no. 11, p. 348, Oct. 2023. [Online]. Available: https://www.mdpi.com/1999-5903/15/11/348

[17] F. Hamidi-Sepehr, M. Sajadieh, S. Panteleev, T. Islam, I. Karls, D. Chatterjee, and J. Ansari, "5G URLLC: Evolution of high-performance wireless networking for industrial automation," *IEEE Commun. Standards Mag.*, vol. 5, no. 2, pp. 132–140, Jun. 2021.

[18] J. Cao, X. Zhu, S. Sun, Z. Wei, Y. Jiang, J. Wang, and V. K. N. Lau, "Toward industrial metaverse: Age of information, latency and reliability of short-packet transmission in 6G," *IEEE Wireless Commun.*, vol. 30, no. 2, pp. 40–47, Apr. 2023.

[19] Y. Ren and V. Friderikos, "Interference aware path planning for mobile robots in mmWave multi cell networks," in *Proc. IEEE 96th Veh. Technol. Conf. (VTC-Fall)*, Sep. 2022, pp. 1–6.

[20] Y. Wang, V. Friderikos, and S. Andraos, "A minmax utilization algorithm for network traffic scheduling of industrial robots," in *Proc. IEEE Int. Conf. Commun. (ICC)*, May 2022, pp. 2936–2941.

[21] (2021). *NIST Advanced Manufacturing Series 300-8, Revision 1–Wireless User Requirements for the Factory Workcell*. [Online]. Available: https://nvlpubs.nist.gov/nistpubs/ams/NIST.AMS.300-8r1-upd.pdf

[22] *3GPP TS 23.288 V18.6.0–Architecture Enhancements for 5G System (5GS) To Support Network Data Analytics Services*. Accessed: Apr. 28, 2025. [Online]. Available: https://www.3gpp.org/ftp/Specs/archive/23_series/23.288/23288-i60.zip

[23] *3GPP TS 23.501 V18.6.0–System Architecture for the 5G System (5GS)*. Accessed: Apr. 28, 2025. [Online]. Available: https://www.3gpp.org/ftp/Specs/archive/23_series/23.501/23501-i60.zip

[24] *3GPP TS 29.517 V18.6.0–Application Function Event Exposure Service*. Accessed: Apr. 28, 2025. [Online]. Available: https://www.3gpp.org/ftp/Specs/archive/29_series/29.517/29517-i60.zip

[25] *Hexa-X-II: D2.3–Interim Overall 6G System Design*. Accessed: Apr. 28, 2025. [Online]. Available: https://hexa-x-ii.eu/wp-content/uploads/2024/07/Hexa-X-II_D2.3-v1.1.pdf

GIANLUCA DAVOLI (Member, IEEE) received the master's degree in telecommunication engineering and the Ph.D. degree in electronics, telecommunication, and information technology engineering from the University of Bologna, Italy, in 2017 and 2021, respectively. He is currently an Assistant Professor with the Department of Electrical, Electronic, and Information Engineering "G. Marconi," University of Bologna. His research work revolves around multiple aspects of softwarization in communication infrastructures, including service orchestration over the cloud continuum, with a focus on the far edge segment. He has been involved in national projects (including PRIN SACHER, PRIN GAUCHO, RESTART-SUPER, and RESTART-RIGOLETTO) and international/industrial ones (including HySIMULED with Thales Alenia Space). He took part in the organizing committee and/or served in the technical program committee of multiple international conferences (including IEEE NetSoft, IEEE NFV-SDN, CNSM, and ICIN).

FEDERICO TONINI (Member, IEEE) received the Ph.D. degree in electronics, telecommunications, and information technology engineering from the Department of Electrical, Electronic, and Information Engineering "G. Marconi," University of Bologna, Italy, in 2019. He is currently a Researcher with the Wireless Laboratory (WiLab), National Inter-University Consortium for Telecommunications (CNIT), Bologna, Italy. His research interests include mobile communication systems, optical network design, and resource optimization techniques.

DAVIDE BORSATTI (Member, IEEE) received the B.S., M.S., and Ph.D. degrees in electronics, telecommunications, and information technologies engineering from the University of Bologna, Italy, in 2016, 2018, and 2022, respectively. He is currently an Assistant Professor with the Department of Electrical, Electronic, and Information Engineering "G. Marconi," University of Bologna. His research interests include NFV, SDN, intent-based networking, MEC, and 5G network slicing.

WINT YI POE received the Ph.D. degree in computer science from the Technical University of Kaiserslautern, Germany, in 2013. She is currently a Principle Researcher with Huawei Technologies, Munich Research Center, Munich, Germany, where her research is focusing on 5G-advanced/6G enabling technologies and network architecture solutions, focusing on AI native multi-functional 6G systems, featuring communication for an efficient, and sustainable support of vertical services. She has several years of experience with standardization activities for 5G/5GA, delivering to 3GPP Releases 15, 16, 17, 18, and 19 in the scope of 3GPP TSG SA WG2 (SA2) and WG5 (SA5). She holds several standard essential patent applications in the area of 5G network architecture and technologies and has authored several conference and journal articles. She has worked with EU funded projects: 5GPPP 5G Exchange (5GEx) Project and 5GPPP 5G Vertical Innovation Infrastructure (5G VINNI) Project.

RICCARDO TRIVISONNO (Senior Member, IEEE) received the M.Sc. and Ph.D. degrees in telecommunications engineering from the University of Bologna, in 2000 and 2005, respectively. He joined Huawei Technologies, in 2011. He is currently the Head of Network Architecture—Research and Standardization—for the Advanced Wireless Technologies Laboratory, Munich Research Center. Over the past ten years, he has been a leading contributor to the definition and the standardization of 5G network architecture and technologies, delivering to 3GPP Releases 15—18—in the areas of architecture modularization, network slicing, network analytics, and QoS—filing more than 100 standard essential patent applications. His research focus shifted to 6G enabling technologies, since 2020. He has been the Chair of 6G-IA pre-standardization WG, since 2020, a Board Member of one6G Association since its foundation, in 2021, and he was elected as the one6G Board Vice-Chair, in 2023.

WALTER CERRONI (Senior Member, IEEE) is currently an Associate Professor in communication networks with the Department of Electrical, Electronic, and Information Engineering "G. Marconi," University of Bologna, Italy. He has co-authored more than 150 articles published in the most renowned international journals, magazines, and conference proceedings. His recent research interests include multiple aspects of control, management, and orchestration of communication network infrastructures, including software-defined networking, network function virtualization, multi-access edge computing, fog computing, service function chaining, and intent-based networking systems. He serves/served as a Series Editor for *IEEE Communications Magazine*, an Associate Editor for IEEE COMMUNICATIONS LETTERS, and the technical program co-chair for IEEE-sponsored international workshops and conferences.